CDF/PHYS/TOP/GROUP/7641
Version 0.3
May 9, 2005

Top Mass Measurement in Dilepton Events using Neutrino ϕ Weighting Method

Giorgio Bellettini[1], Julian Budagov[2], Guram Chlachidze[2], Vladimir Glagolev[2], Fiodar Prakoshyn[2], Alexei Sissakian[2], Igor Suslov[2], George Velev[3]

Abstract

We report on a measurement of the top quark mass in the dilepton events using the neutrino ϕ weighting method. The integrated luminosity of the data sample is 335 pb^{-1}. 33 dilepton candidates were obtained within the event selection cuts from the dilepton cross section group. These events were reconstructed according to the $t\bar{t}$ hypothesis and fitted as a superposition of signal and combined background. The constrained fit returned a mass $M_{top} = 170.0 \pm^{9.7}_{8.9}$ (stat) GeV/c^2. The estimate of systematic error is ± 4.0 GeV/c^2.

[1]INFN and Department of Physics, University of Pisa

[2]JINR, Dubna

[3]Fermilab

1 Introduction

In this note, we present a top mass measurement in the dilepton channel using the neutrino ϕ weighting algorithm. The adopted method was proposed for the first time in Run 1 [1]. The data sample includes data collected between March 2002 and Auguist 2004 corresponding to a total integrated luminosity of 335 pb^{-1}.

Data samples were produced using the 5.3.1 version of Production, and Monte-Carlo (MC) samples were produced using version 5.3.3 of CdfSim and Production. CDF offline version 5.3.3_nt was used for the event selection and further analysis.

Top specific jet-to-parton corrections extracted from MC dilepton events were applied after level-5 jet corrections. No use is made of b-tag information in this analysis.

2 Brief Description of The Method

2.1 General Notes

The top mass value for each event is returned from a kinematic event reconstruction procedure. This procedure is similar to the one used in the lepton+jets case [2]. In brief, event reconstruction is the result of minimization of the chisquare functional (χ^2) by the MINUIT routines. This chisquare functional has resolution terms related to the measured physical variables and constrained terms to take into account kinematic equations.

In contrast to the lepton+jets mode, for the dilepton case due to the existence of two neutrinos we have a non-constrained kinematics. The number of independent variables is one more than the number of kinematic constraints ($-1C$ kinematics). Obviously, it is impossible to pick up directly only one solution per event. We must assume some of the event parameters ($\vec{R}$) as known in order to constrain the kinematics and then vary the $\vec{R}$ to determine the variety of solutions. In addition, every solution must have a weight attached to it.

The minimal requirement in the case of $-1C$ kinematics is to use a two dimensional vector as $\vec{R}$. For our analysis we chose the azimuthal angles of the neutrino momenta $\vec{R} = (\phi_{\nu 1}, \phi_{\nu 2})$ and we create a net of solutions in the $(\phi_{\nu 1}, \phi_{\nu 2})$ plane.

For every point of the $(\phi_{\nu 1}, \phi_{\nu 2})$ plane we have 8 solutions. Two of them are generated due to the different possibilities to associate the two charged leptons to the two leading jets (which are supposed to be b-jets). The four other solutions are generated from the possibility for every neutrino to have two p_z momenta of opposite sign satisfying the $t\bar{t}$ kinematics. We select the minimal χ^2 solution for every point of the net for further use in our analysis.

Using the χ^2 value from a minimization we weight the selected solutions by $\exp(-\chi^2/2)$. This is done in order to suppress the solutions which have worse compliance with the fit hypothesis.

The final extraction of the top quark mass from a sample of dilepton candidates is provided by the likelihood fit. The expected signal and background distributions are obtained using Monte Carlo samples with detector simulation.

2.2 The χ^2 form

The minimized χ^2 is as follows:

$$\chi^2 = \sum_{l=1}^{2} \frac{(P_T^l - \widetilde{P_T^l})^2}{{\sigma_{P_T}^l}^2} + \sum_{j=1}^{2} \frac{(P_T^j - \widetilde{P_T^j})^2}{{\sigma_{P_T}^j}^2} + \sum_{i=x,y} \frac{(UE^i - \widetilde{UE^i})^2}{{\sigma_{UE}^i}^2} +$$

$$+ \frac{(M_{l_1\nu_1} - M_W)^2}{\Gamma_{M_W}^2} + \frac{(M_{l_2\nu_2} - M_W)^2}{\Gamma_{M_W}^2} + \frac{(M_{j_1 l_1 \nu_1} - \widetilde{m_t})^2}{\Gamma_{M_t}^2} + \frac{(M_{j_2 l_2 \nu_2} - \widetilde{m_t})^2}{\Gamma_{M_t}^2} \quad (1)$$

The variables with a tilde sign refer to the output of the minimization procedure, whereas P_T and UE (underlying energy) represent measured values corrected for known detector and physics effects. $\widetilde{m_t}$ is the fit parameter giving the reconstructed top mass for the combination being considered.

The first sum runs over the primary leptons. The second sum is over two leading jets with level-5-corrected $E_T > 15$ GeV and $|\eta| < 2.5$. The 68% CL of jet response obtained from top specific jet corrections (see section 4.1) is used as a jet P_T resolution in the denominator of this term. The third sum is over the transverse components of the unclustered energy[1]. Here we take $M_W = 80.41$ GeV/c^2 and $\Gamma_{M_W} = 2.06$ GeV/c^2, $\Gamma_{M_t} = 2.5$ GeV/c^2 as the W and top natural widths.

2.3 Scanning of the $(\phi_{\nu 1}, \phi_{\nu 2})$ plane

To provide $1C$ fit minimization by (1) we must take two additional event parameters as known. Let they be $\phi_{\nu 1}$ and $\phi_{\nu 2}$ [1].

For one point in the $(\phi_{\nu 1}, \phi_{\nu 2})$ plane we can write a linear system:

$$\begin{cases} P_T^{\nu 1} \cdot cos(\phi_{\nu 1}) + P_T^{\nu 2} \cdot cos(\phi_{\nu 2}) = \not{E}_{Tx} \\ P_T^{\nu 1} \cdot sin(\phi_{\nu 1}) + P_T^{\nu 2} \cdot sin(\phi_{\nu 2}) = \not{E}_{Ty} \end{cases} \quad (2)$$

[1]In (1) the additional jets are taken into account as part of the unclustered energy. These jets are determined with the requiments $E_T > 8$ GeV after level 5 jet corrections and $|\eta| < 2.5$. The level 5 corrected E_T of these additional jets are added to the initial UE. This was done in order to avoid the jet corrections for the underlying event and for out-of-cone energy (level 6 and 7 corrections) which are not yet well understood for Run 2. Details are in [4].

Solving the linear system (2) we obtain:

$$\begin{cases} p_x^{\nu 1} \equiv P_T^{\nu 1} \cdot cos(\phi_{\nu 1}) = \frac{\not{E}_{Tx} \cdot sin(\phi_{\nu 2}) - \not{E}_{Ty} \cdot cos(\phi_{\nu 2})}{sin(\phi_{\nu 2} - \phi_{\nu 1})} \cdot cos(\phi_{\nu 1}) \\ p_y^{\nu 1} \equiv P_T^{\nu 1} \cdot sin(\phi_{\nu 1}) = \frac{\not{E}_{Tx} \cdot sin(\phi_{\nu 2}) - \not{E}_{Ty} \cdot cos(\phi_{\nu 2})}{sin(\phi_{\nu 2} - \phi_{\nu 1})} \cdot sin(\phi_{\nu 1}) \\ p_x^{\nu 2} \equiv P_T^{\nu 2} \cdot cos(\phi_{\nu 2}) = \frac{\not{E}_{Tx} \cdot sin(\phi_{\nu 1}) - \not{E}_{Ty} \cdot cos(\phi_{\nu 1})}{sin(\phi_{\nu 1} - \phi_{\nu 2})} \cdot cos(\phi_{\nu 2}) \\ p_y^{\nu 2} \equiv P_T^{\nu 2} \cdot sin(\phi_{\nu 2}) = \frac{\not{E}_{Tx} \cdot sin(\phi_{\nu 1}) - \not{E}_{Ty} \cdot cos(\phi_{\nu 1})}{sin(\phi_{\nu 1} - \phi_{\nu 2})} \cdot sin(\phi_{\nu 2}) \end{cases} \tag{3}$$

For each point in the $(\phi_{\nu 1}, \phi_{\nu 2})$ plane it is possible to do a $1C$ fit minimization of (1) using (3). The next step is to scan the $(\phi_{\nu 1}, \phi_{\nu 2})$ plane and create a net of solutions. We note that the solutions of (3) are not defined in the case of $sin(\phi_{\nu 1} - \phi_{\nu 2}) = 0$ or $\phi_{\nu 1} - \phi_{\nu 2} = k \cdot \pi$, but this is no limitation in practice. The net of points is chosen with the requirement to avoid the lines $\phi_{\nu 1} - \phi_{\nu 2} = k \cdot \pi$.

We do not need to cover full $(\phi_{\nu 1}, \phi_{\nu 2})$ plane by the net. It is enough to use the points in quadrant $(0 < \phi_{\nu 1} < \pi, 0 < \phi_{\nu 2} < \pi)$. We will have the same components of neutrino's momentum $p_{x,y}^{\nu 1,\nu 2}$ by (3) for $\phi'_{\nu 1,\nu 2} = \phi_{\nu 1,\nu 2} + \pi$ and as consequence the same results from fit minimization for four points $(\phi_{\nu 1}, \phi_{\nu 2})$, $(\phi_{\nu 1} + \pi, \phi_{\nu 2})$, $(\phi_{\nu 1}, \phi_{\nu 2} + \pi)$, $(\phi_{\nu 1} + \pi, \phi_{\nu 2} + \pi)$. It is also significant to note that $P_T^{\nu 1,\nu 2}$ will only change sign by adding π to $\phi_{\nu 1,\nu 2}$. So we can write:

$$\phi'_{\nu 1,\nu 2} = \phi_{\nu 1,\nu 2} + \pi \implies p'^{\,\nu 1,\nu 2}_{x,y} = p_{x,y}^{\nu 1,\nu 2} \text{ and } P'^{\,\nu 1,\nu 2}_{T} = -P_T^{\nu 1,\nu 2}$$

Thus the physical solution exists for one of the four points only. This point is determined by the conditions $P_T^{\nu 1} > 0$ and $P_T^{\nu 2} > 0$. The solutions from other points are unphysical and are the "mirror reflections" of the physical solution.

The net is chosen to have 12×12 points. As it was noticed above for every point we have 8 solutions from the ambiguity of the $p_z^{\nu 1,\nu 2}$ and jet assignment. For every event we have 1152 $1C$ minimizations with an output χ^2_{ijk} and m^{rec}_{ijk} $(i = 1, 12;\ j = 1, 12;\ k = 1, 8)$. We selected the minimal χ^2_{ijk} for every point $(i, j$-fixed; $k = 1, 8)$. The final output from this procedure was an array of 144 χ^2_{ij} and m^{rec}_{ij}.

2.4 Weighting of the 144 event solutions

Having the χ^2's from a minimization gives us the possibility to weight the solutions by $exp(-\chi^2/2)$. The overall normalization of the event probability density distribution (p.d.d.'s) is chosen to be one. The expression for the weight is:

$$w_{ij} = \frac{exp(-\chi^2_{ij}/2)}{\sum_{i=1}^{12} \sum_{j=1}^{12} exp(-\chi^2_{ij}/2)} \tag{4}$$

2.5 Templates

Our templates are the sum of the p.d.d.'s for each event. The mass-dependent template function $f_s(m_t|M_{top})$ and the background template function $f_b(m_t)$ are determined as follows.

A set of templates for different input top masses is parametrized as a sum of a Gamma function and of a Gaussian comprising 6 parameters that depend linearly on the top mass.

$$f_s(m_t|M_{top}) = \frac{(1-p_6)}{\sqrt{2\pi}p_5} e^{-0.5(\frac{m_t-p_4}{p_5})^2} + \frac{p_6 p_3^{(1+p_2)}}{\Gamma(1+p_2)}(m_t-p_1)^{p_2} e^{-p_3(m_t-p_1)} \quad (5)$$

The parameters of the Gaussian and Gamma distributions are themselves linear functions of the input top mass M_{top}:

$$p_k = \alpha_k + \alpha_{k+6} \cdot M_{top} \quad (6)$$

The set of signal MC templates is fitted to obtain the 12 α_k parameters.

The background template is parameterized with the Gamma function, and with M_{top}-independent parameters.

2.6 Likelihood form

We use a maximum likelihood method to extract the top quark mass by comparing the reconstructed top mass distribution of the data with the superposition of signal and background. The used likelihood form is as follows:

$$L = L_{shape} \cdot L_{backgr} \cdot L_{param}; \quad (7)$$

In *Gen.4* we used:

$$L_{shape} = \prod_{n=1}^{N_{evn}} \prod_{i=1}^{12} \prod_{j=1}^{12} (\beta_s \cdot f_s(m_{ij}^{rec}|M_{top}) + (1-\beta_s) \cdot f_b(m_{ij}^{rec}))^{w_{ij}} \quad (8)$$

where β_s is the expected signal fraction in the dilepton data sample. Also the additional terms were added to constrain number of the background events and to constrain $\vec{\alpha}$, $\vec{\beta}$ parameters, obtained from the signal and background template parameterization:

$$L_{backgr} = exp(\frac{-(N_b - (1-\beta_s) \cdot N_{evn})^2}{2\sigma_{N_b}^2}) \quad (9)$$

$$L_{param} = exp\{-0.5[(\vec{\alpha} - \vec{\alpha_0})^T U^{-1} (\vec{\alpha} - \vec{\alpha_0}) + (\vec{\beta} - \vec{\beta_0})^T V^{-1} (\vec{\beta} - \vec{\beta_0})]\}. \quad (10)$$

Here U and V are the covariance matrices for $\vec{\alpha_0}$ and $\vec{\beta_0}$ respectively.
This likelihood form was tested and found to work well in Run 1 analysis [1].

2.7 MINUIT procedure

Our procedure was based on the $l+jets$ development code of the top mass group. A new code, which corresponds to the dilepton event kinematics, was added to *TopMassFitModule*. Top specific jet corrections, which were extracted from Monte Carlo dilepton events, are applied to the supposed b-jets.

2.8 MC studies

Having adopted for dilepton kinematics the *TopMassFitModule* we performed some studies on MC events in Gen.4 to check the performance of our method. For this study we used the official MC Herwig samples with different input top mass values. We required the events to be dileptons at HEPG level and to pass our selection cuts. An additional requirement was the matching within a cone radius of 0.4 for every primary lepton in the event with a HEPG lepton from the $t\bar{t}$ decay chain. Owing to this additional requirement we were able to associate the HEPG bank neutrinos with the primary leptons.

Examples of χ^2 distributions in the $(\phi_{\nu 1}, \phi_{\nu 2})$ plane are presented in Fig. 1. The number of bins in these histograms is 24×24. In each bin only one χ^2 from χ^2_{ij} array is set as a weight. Large weights are set for bins with unphysical solutions. The region of expected neutrino values can be clearly seen in these histograms. The "genuine" (generated) neutrino values are shown as the color marker.

In order to inspect how effective our weight determination is we looked at 2D distributions of $\phi^{MC}_{\nu 1} - \phi^{i,j}_{\nu 1}$, $\phi^{MC}_{\nu 2} - \phi^{i,j}_{\nu 2}$ variables with weights w_{ij} . These distributions for several input top masses are presented in Fig. 2.

2.9 Method optimization

To improve resolution we optimized our method selecting more meaningful information from our event probability density distribution. The idea is to select one top mass value per event instead of using all 144 masses.

The shape likelihood now is:

$$L_{shape} = \prod_{n=1}^{N_{evn}} (\beta_s \cdot f_s(m^{rec}_{ij}|M_{top}) + (1-\beta_s) \cdot f_b(m^{rec}_{ij}))^{w_{ij}} \tag{11}$$

We applied a cut on our probability density distribution (as a fraction of bin content at MPV) and selected the average mass for the bins passed this cut. This cut was optimized with respect to the expected statistical errors.

The discriminator Level (DL) was varied in the interval from 0.0 to 0.5 of the bin content at MPV of the pdd distribution. The Figures(3, 4, 5) show the results from the MC pseudo-experiments. Points at DL=-0.1 obtained with the use of whole pdd (144 masses per event). We can conclude that DL = 0.3 gives the better resolution and we expect 25 % improvement in resolution with this modification.

2.10 ϕ segmentation study

We studied the effect of neutrino ϕ-plane segmentation on the resolution of mass templates. We produced MC templates for three different grids (6x6, 12x12 and 24x24). The templates are shown in Fig. 6.

The Fig. 7 shows the template RMS for different ϕ segmemtation. We can conclude that 12x12 and 24x24 segmentation give the same resolution for mass templates.

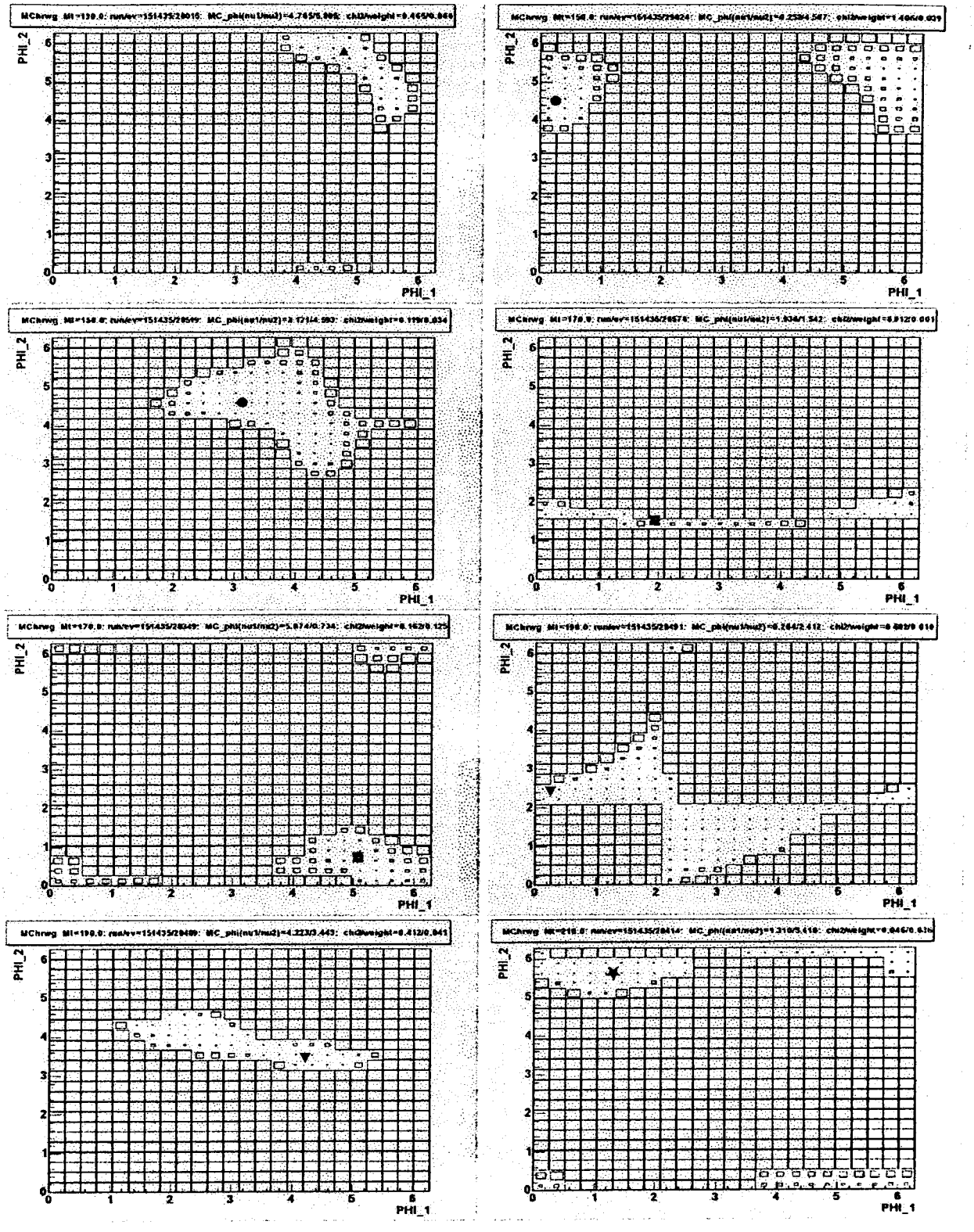

Figure 1: χ^2 distributions in the $(\phi_{\nu 1}, \phi_{\nu 2})$ plane for a number of simulated dilepton events. The region of expected neutrino values can be seen. The "genuine" neutrino values are shown as the color marker.

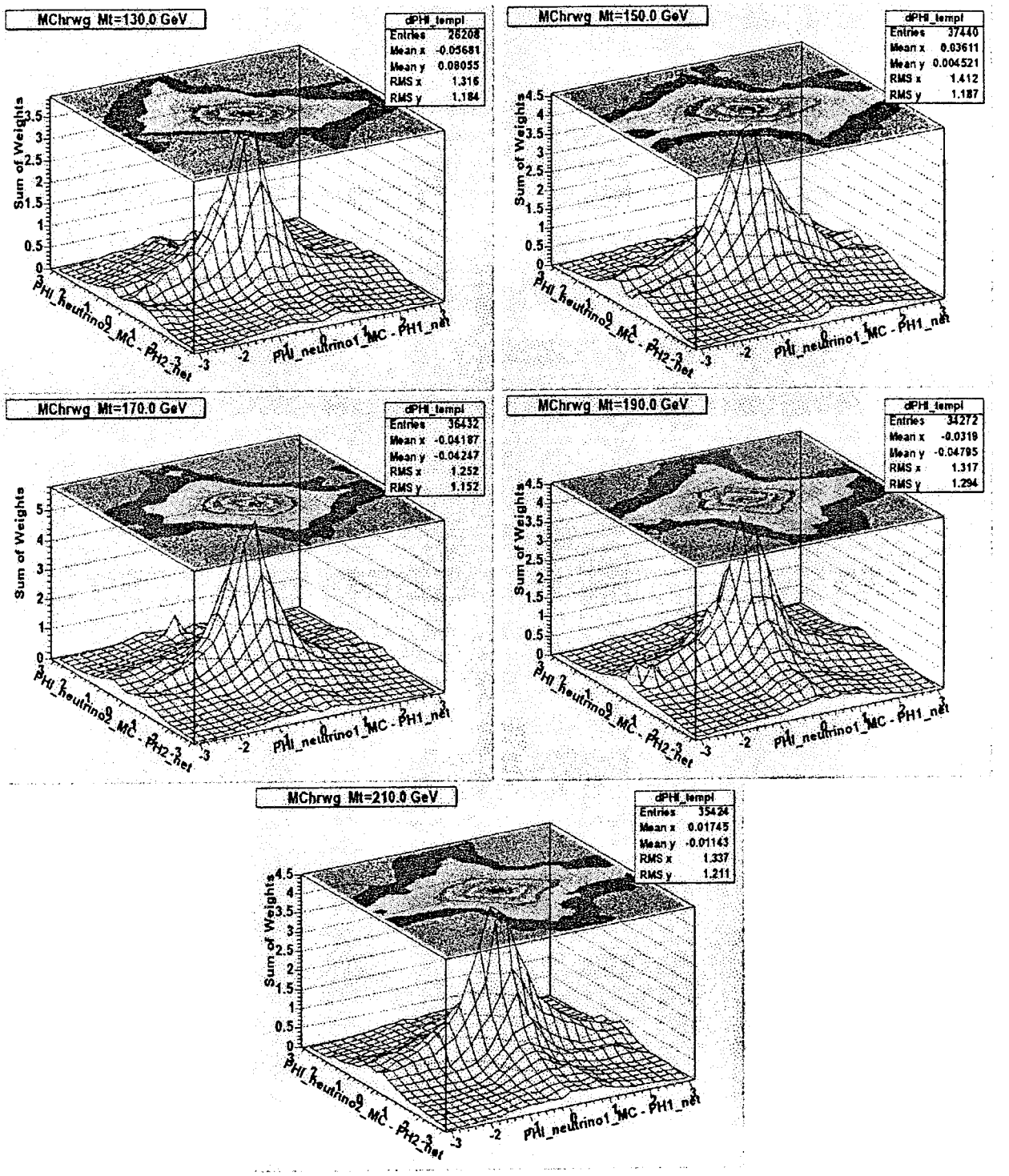

Figure 2: 2D distributions of $\phi_{\nu 1}^{MC} - \phi_{\nu 1}^{i,j}$, $\phi_{\nu 2}^{MC} - \phi_{\nu 2}^{i,j}$ with weights w_{ij}.

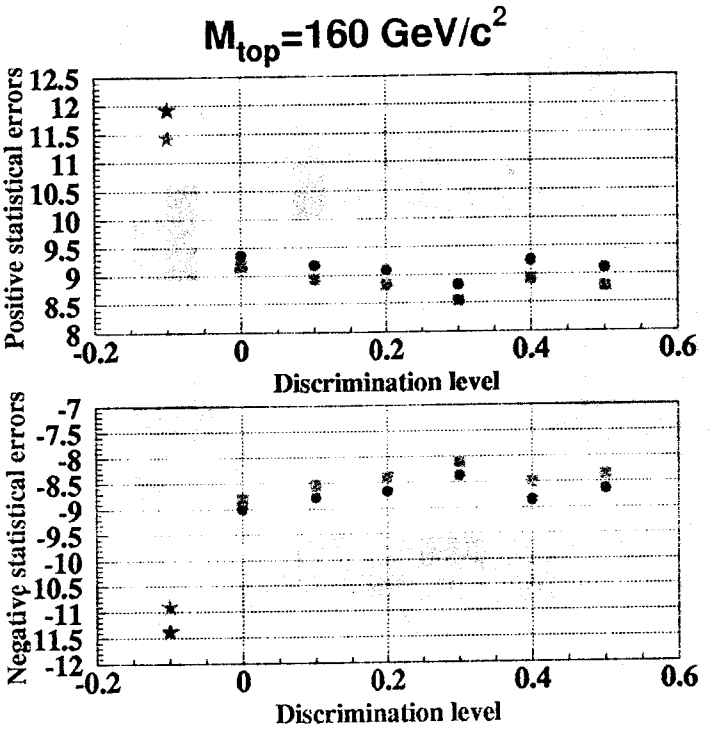

Figure 3: Mean/Median from statistical error distribution vs. cut (DL). Top mass 160 GeV

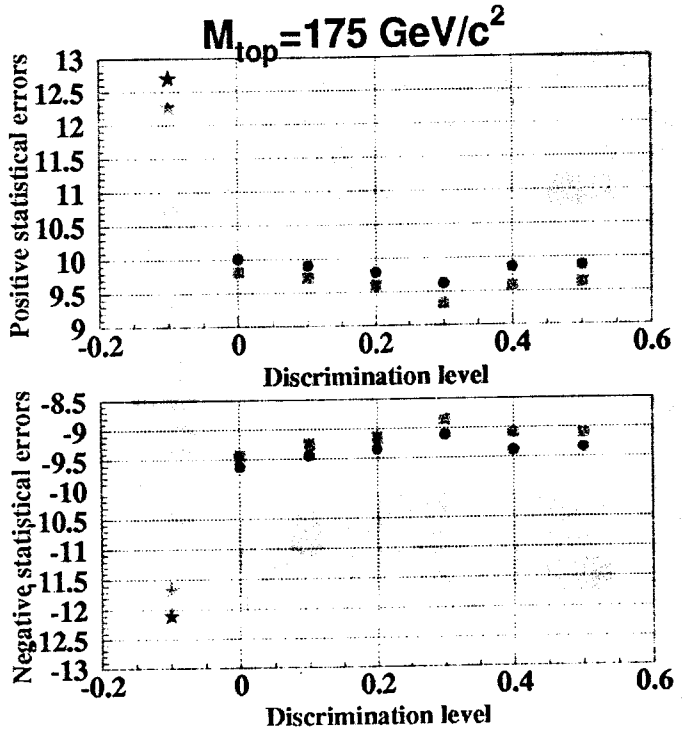

Figure 4: Mean/Median from statistical error distribution vs. cut (DL). Top mass 175 GeV

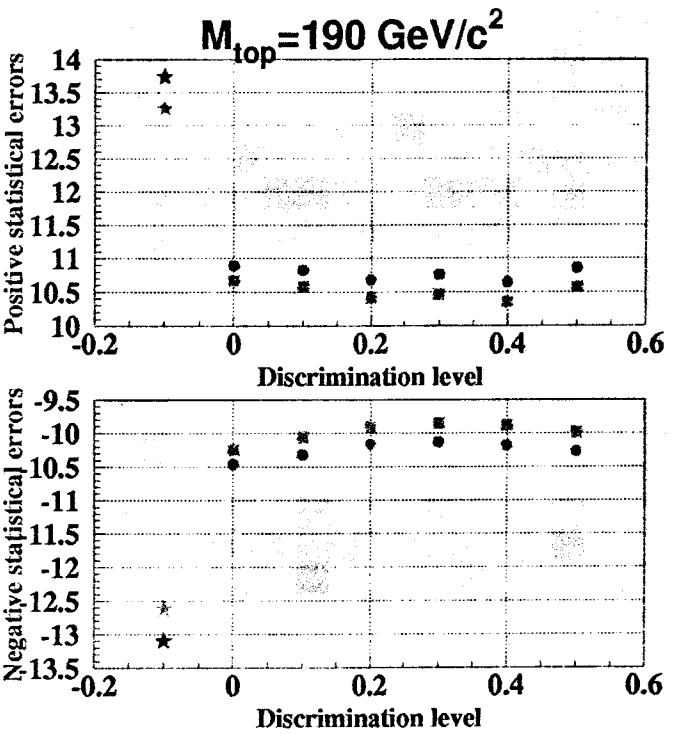

Figure 5: Mean/Median from statistical error distribution vs. cut (DL). Top mass 190 GeV

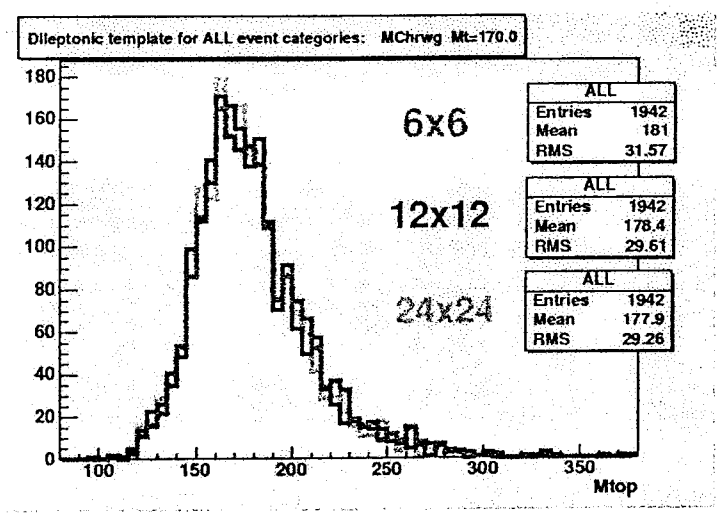

Figure 6: MC mass templates for different neutrino ϕ-plane segmentation for top mass 170 GeV

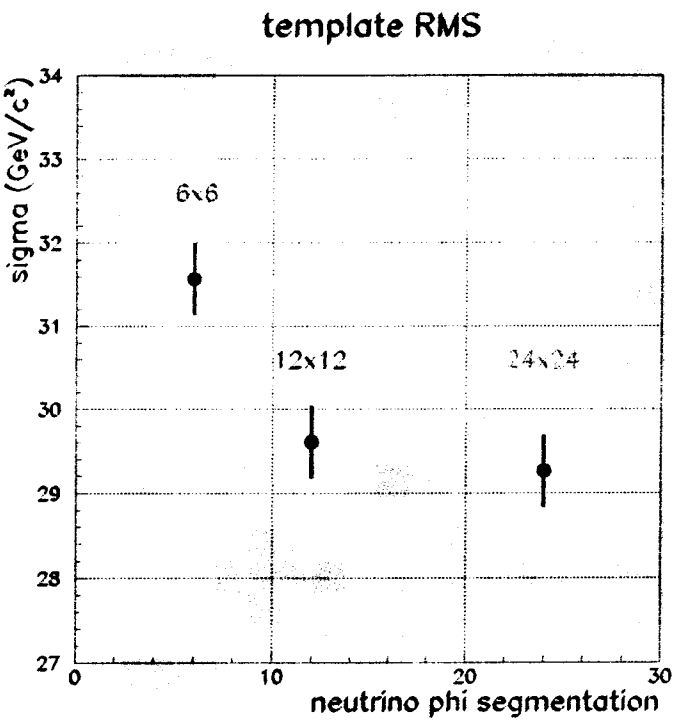

Figure 7: Sigma of templates vs. different neutrino phi plane segmentation

3 Event Selection

The event selection for this analysis is **DIL** type and performed as described on the dilepton cross section group web page:

`http://cdfrh0.grid.umich.edu/%7Etecchio/topntuple/DIL_topntuple.html`

4 Jet Corrections

As a first step for correcting the raw jet energy the inclusive jet corrections as presently recommended by the jet corrections group[1] were applied. For both event selection cuts and mass extraction we used level-5-corrected jets. In addition the top specific corrections (TSJC) were applied also to take into account the non-flat P_T spectrum of jets from $t\bar{t}$-decays and the different fragmentation functions of b-jets. An appropriate η-dependence is taken into account in these top-specific corrections since the P_T spectrum of jets from top decays is strongly η-dependent. Description of these top-specific corrections is given below.

[1] This is the *JetUser* package tagged as *jetCorr04b*

4.1 Improvement of Top Specific Jet Corrections

For this analyses we have decided to improve our MPV top specific jet corrections described in [3]. Instead of using most probable values (MPV) now we are using so called MIN68 values. MIN68 for the $(P_T^{parton} - P_T^{jet})/P_T^{jet}$ *vs* P_T^{jet} distribution is obtained by minimizing 68% CL coverage.

The obtained resolutions for different type of TSJC and for different top masses are shown in Figures 8, 9, 10.

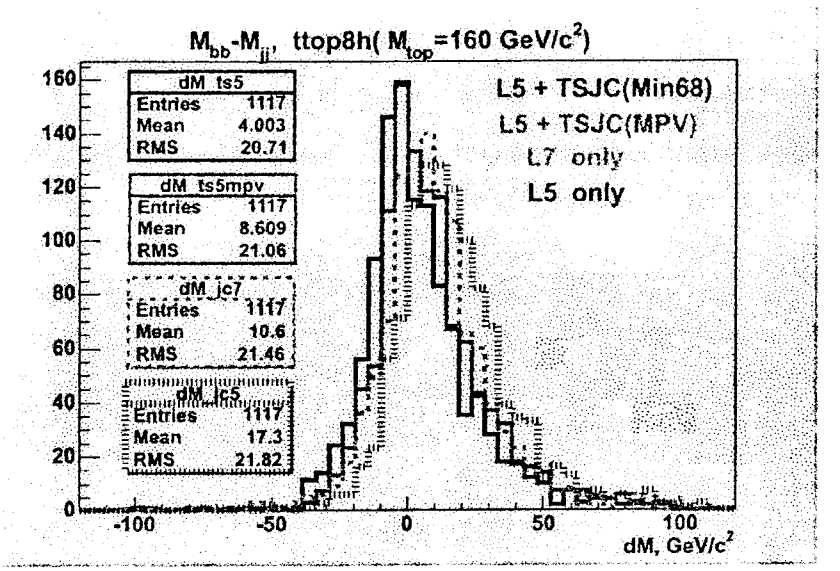

Figure 8: Resolution for effective mass of 2 b-jets obtained with different type of TSJC for Top mass 160 GeV

We made a choise of MIN68 as providing the better resolution.

4.2 Top Specific Jet Corrections

We developed the top specific jet corrections and used them in our analysis. The overall technical description of top-specific corrections can be found in CDF notes [8, 7]. Some properties of top specific corrections in our analysis are as follow:

- extracted from dilepton HEPG events;
- obtained on MC sample *ttophl* M_{top} 178 GeV range
- top specific corrections were defined independently in three $|\eta|$ ranges: $|\eta| < 0.7$; $0.7 < |\eta| < 1.3$; $1.3 < |\eta| < 2.5$.
- starting from *level*5 jet corrections;
- DIL selection cuts were used.

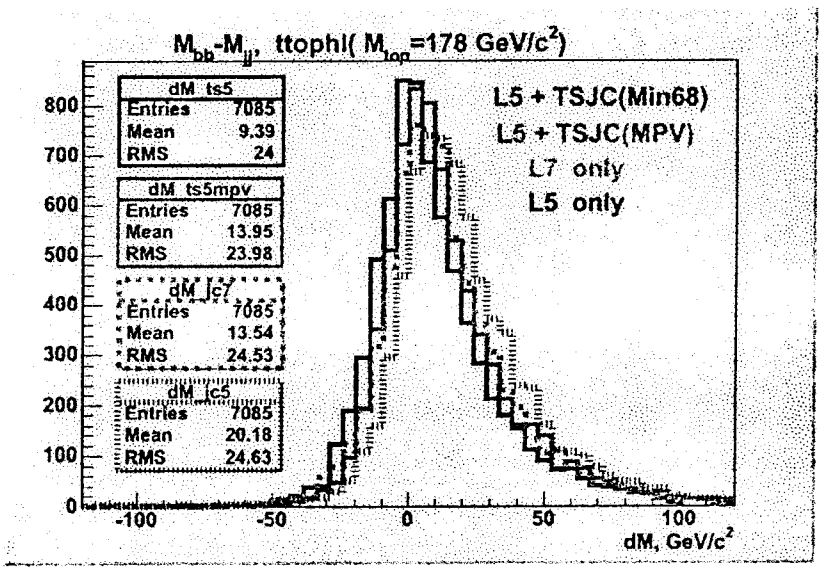

Figure 9: resolution for effective mass of 2 b-jet obtained with different type of TSJC for Top mass 178 GeV

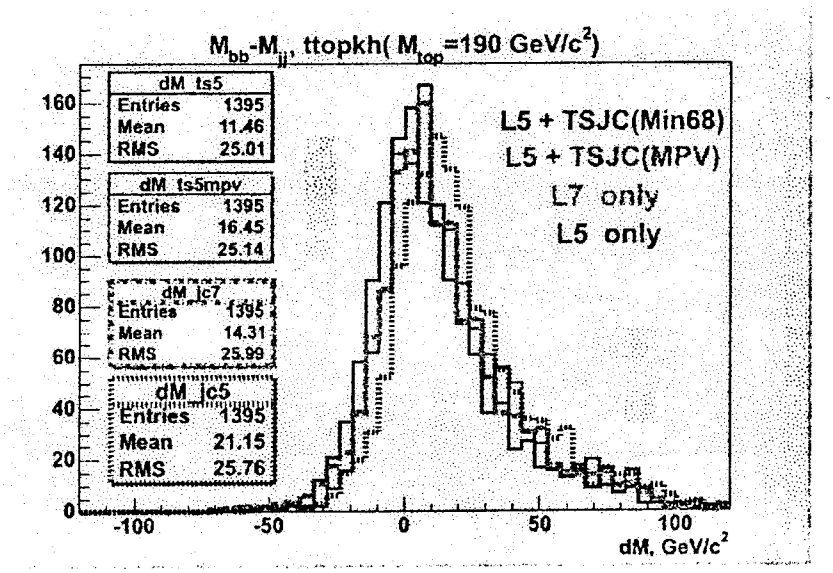

Figure 10: resolution for effective mass of 2 b-jet obtained with different type of TSJC for Top mass 190 GeV

In brief, these corrections were extracted from MC samples as follows:

1. reconstruct jets in a cone of radius R=0.4 and correct their energy with *level*5 jet corrections;
2. select jets of *level*5 corrected energy $E_T > 15$ GeV and look for a match between jets and b quarks within a cone of radius R=0.4 around the b quark direction;
3. plot the $(P_T^{parton} - P_T^{jet})/P_T^{jet}$ *vs* P_T^{jet} for the b jets;
4. slice the scatter plots in bins of P_T^{jet} and project on the x-axis;
5. retrieve the MIN68 and CL68 of each of the slices, and fit them as a function of P_T^{jet}.

The obtained fit parameters and the fit functions form for different $|\eta|$ ranges are shown in Figs. 11, 12, 13.

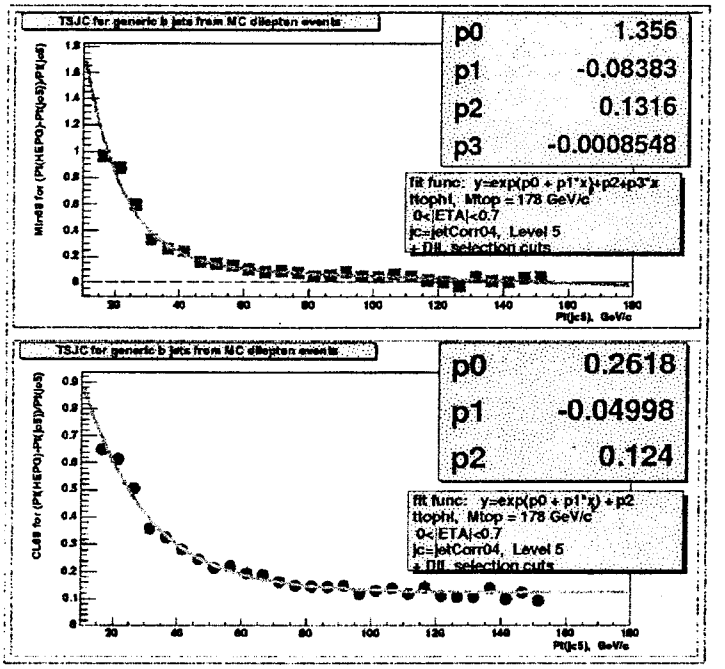

Figure 11: MIN68(above) and CL68(below) of $(P_T^{parton} - P_T^{jet})/P_T^{jet}$ distributions as a function of P_T^{jet}. Jets are corrected with level 5 corrections; $|\eta| < 0.7$. The fit results are also shown as continous curves.

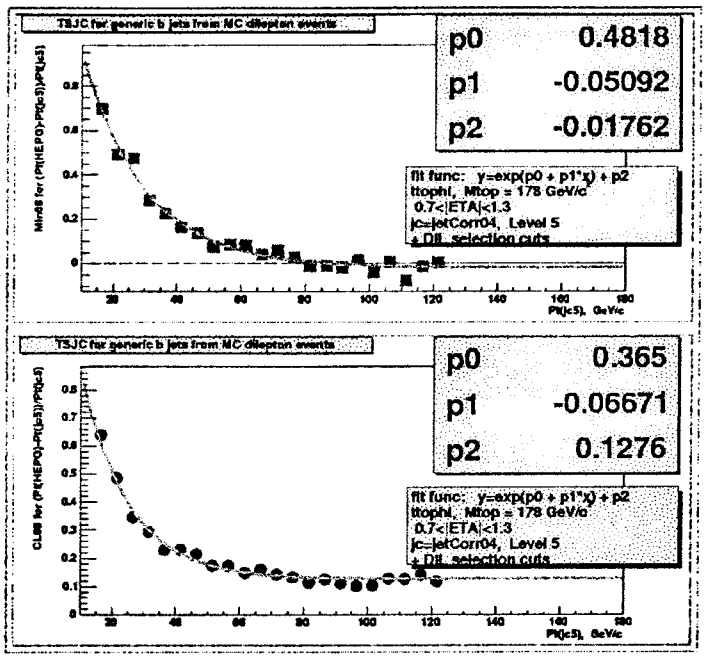

Figure 12: MIN68(above) and CL68(below) of $(P_T^{parton} - P_T^{jet})/P_T^{jet}$ distributions as a function of P_T^{jet}. Jets are corrected with level 5 corrections; $0.7 < |\eta| < 1.3$. The fit results are also shown as continous curves.

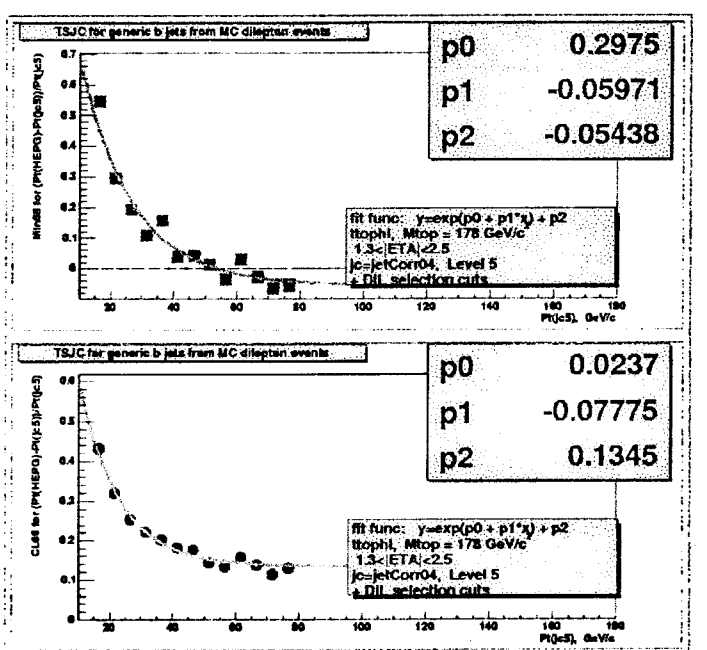

Figure 13: MIN68(above) and CL68(below) of $(P_T^{parton} - P_T^{jet})/P_T^{jet}$ distributions as a function of P_T^{jet}. Jets are corrected with level 5 corrections; $1.3 < |\eta| < 2.5$. The fit results are also shown as continous curves.

5 Templates

5.1 Monte Carlo Signal Templates

The official Herwig MC samples were used. The signal templates for input top masses in the 140÷230 GeV range were created in 5 GeV steps. Then the obtained set of templates was parameterized by (5). The examples of our templates are presented in Figs. 14.

5.2 Background template

We used for background processes official Gen.5 MC samples ($WZ \to ll$, $WW \to ll$, Drel-Yan, $Z \to \tau\tau$ and "fake" lepton).

The obtained templates (Fig. 16) for these processes were combined together according to the expected number of events as derived by the *ttbar* cross section group. The numbers we took from the Table at Fig 15.

The result for the combined background template is shown on the same Fig. 16, right lower plot.

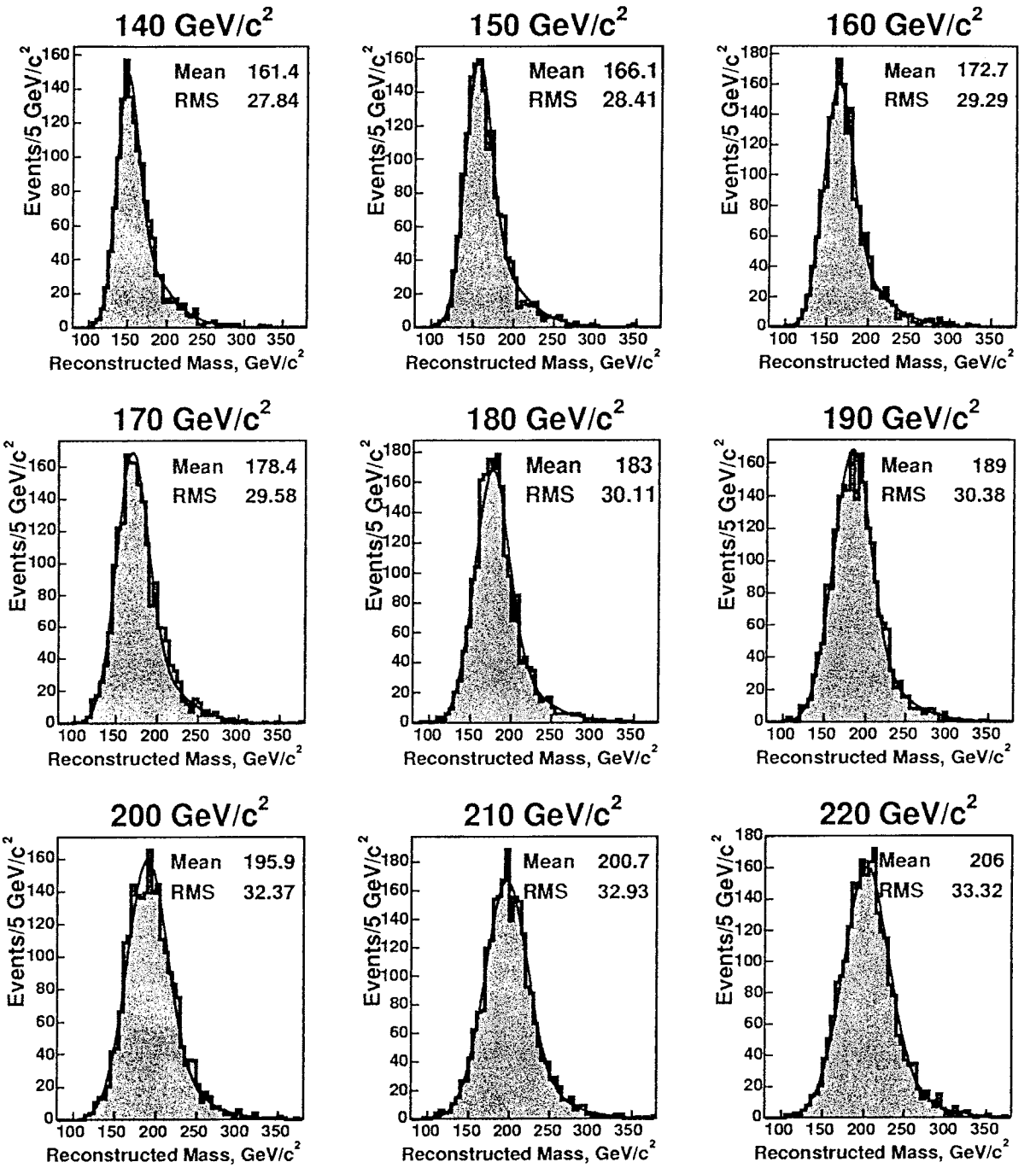

Figure 14: Signal templates for top masses in the 140÷220 GeV/c^2 range. The curves from the global fit (5) are also shown.

Background

Monica Tecchio April 6

Top Dilepton Selection Background status report

	0j	1j	2j	HT+OS
WW/WZ	12.9 +- 0.5	4.1 +- 0.2	1.8 +- 0.2	1.07 +- 0.17
DY	6.1 +- 4.8	5.4 +- 3.6	2.3 +- 1.2	1.7 +- 0.6
Z->ττ	0.2 +- 0.02	1.1 +- 0.2	0.8 +– 0.2	0.44 +- 0.01
Fakes	**9.6 +- 3.8**	**6.5 +- 2.6**	**4.0+-1.6**	**1.74 +-0.70**
Total background	**28.7 +- 6.2**	**17.1 +- 4.4**	**8.9 +- 1.8**	**4.9 +- 0.9**
Top (6.7 pb)	0.04 +- 0.003	1.23 +- 0.10	10.4 +- 0.8	9.76 + 0.78
Total SM 5.3.3	28.7 +- 6.2	18.3 +- 4.4	19.3 +- 2.5	14.6 +- 1.0
Data 5.3.3	**22**	**18**	**23**	**18**

We rescale 193 pb^{-1} -> 335 pb^{-1}

Figure 15: background numbers from x-section group

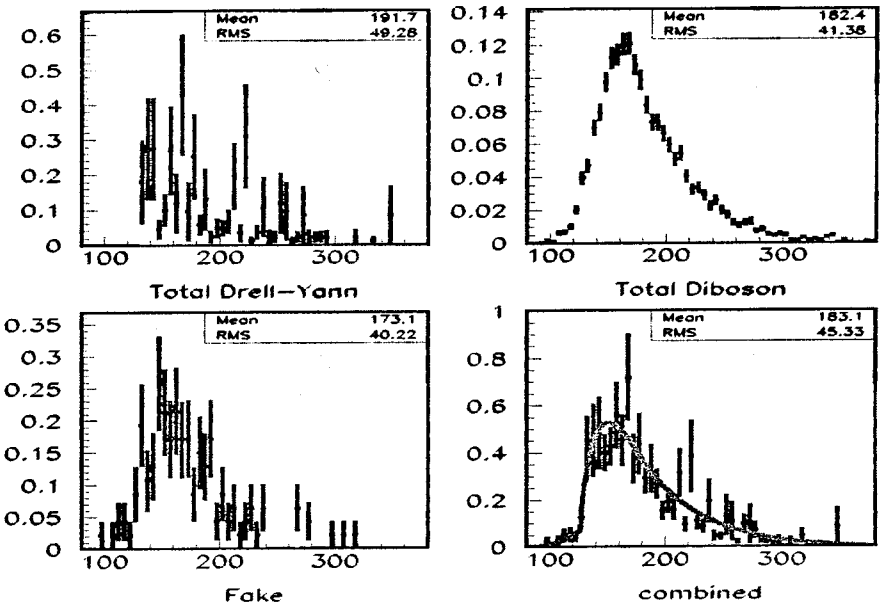

Figure 16: Templates of background processes Drell-Yan, Diboson, "fake" lepton. Lower right plot shows the combined background.

6 Results from pseudo-experiments

We checked whether the fit with likelihood form (7) was able to return the correct mass by performing the "sanity check" pseudo-experiments for different input top mass values. The overall number of events in the pseudo-experiments was 33 with expected number of background 8.5±1.6 events. The output m_{top} (mean of Gaussian fit) vs. input M_{top} is shown in Fig. 17. A linear fit yielded a slope of 1.01±0.01. The mean and width of the pull distributions as a function of input top mass are shown in Fig. 18.

7 Blind test results

Before "opening the box" with data we performed our analysis on the "blind" MC samples. The difference between extracted and true mass values for different samples in random order are shown in Fig. 19.

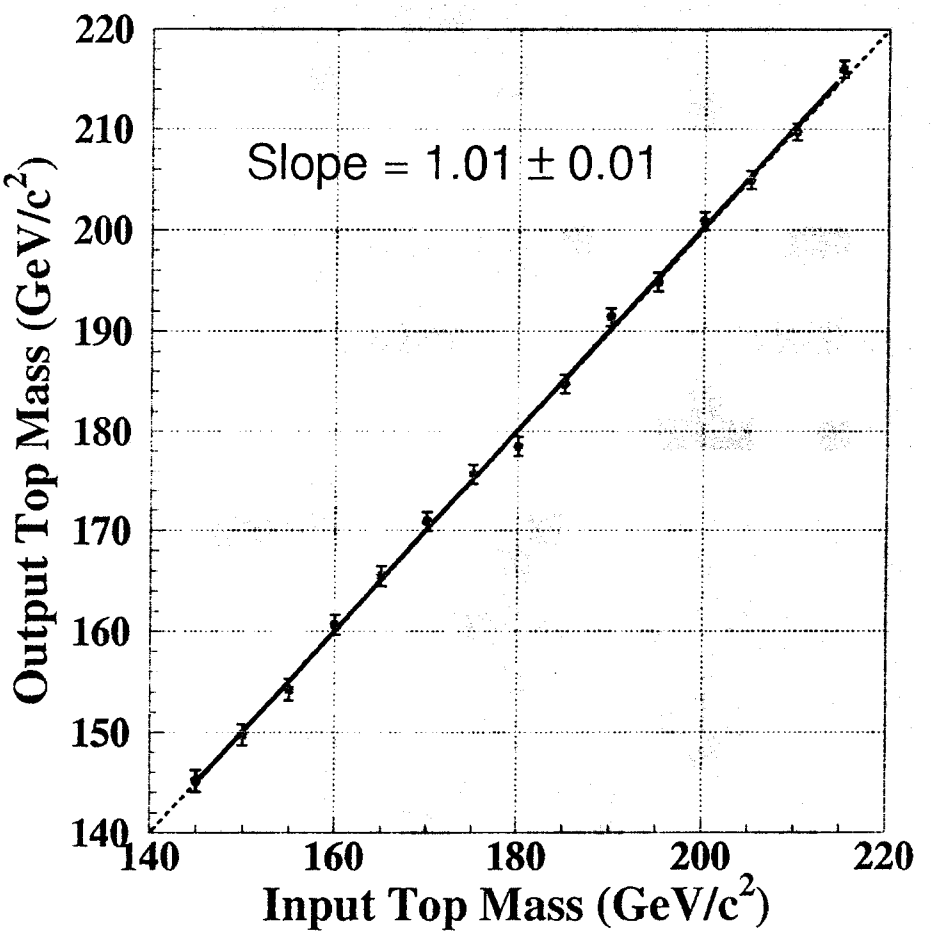

Figure 17: The extracted top mass as a function of input mass. The result of a linear fit is also shown.

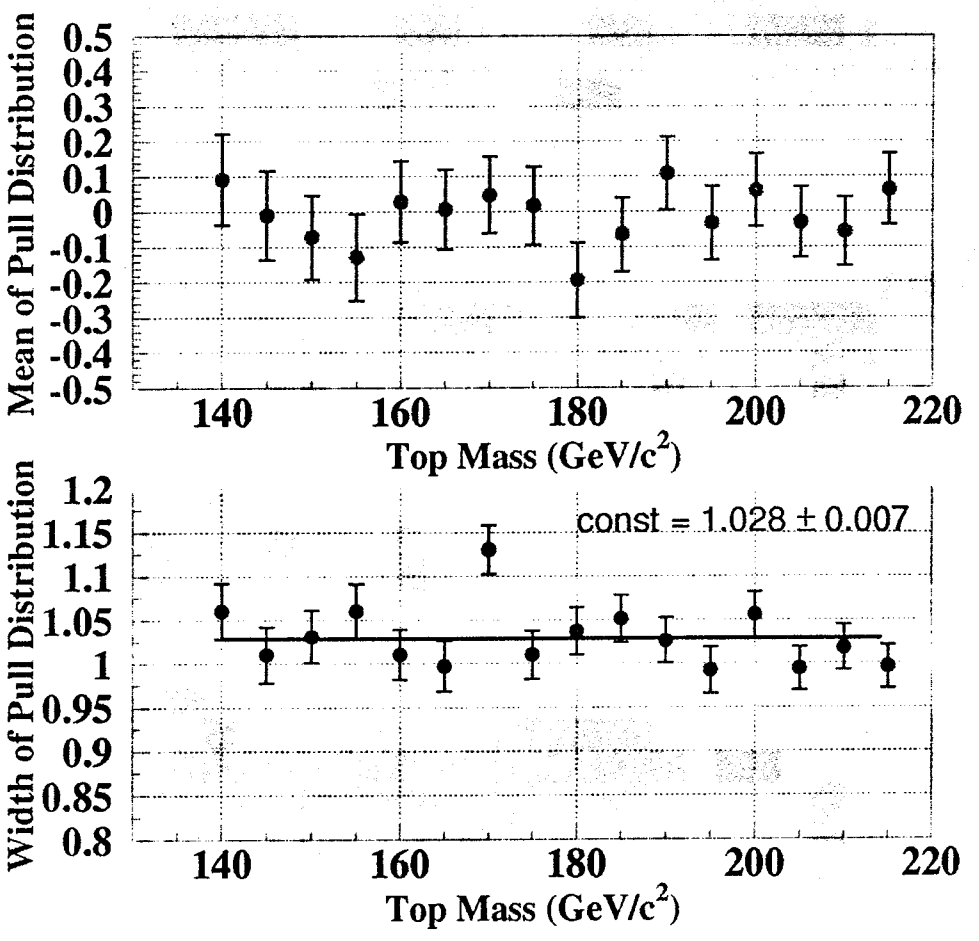

Figure 18: Mean (above) and σ (below) of pull distributions determined from the pseudo-experiments as a function of input top mass.

Blind sample results

- Signal and background mixed in expected portions

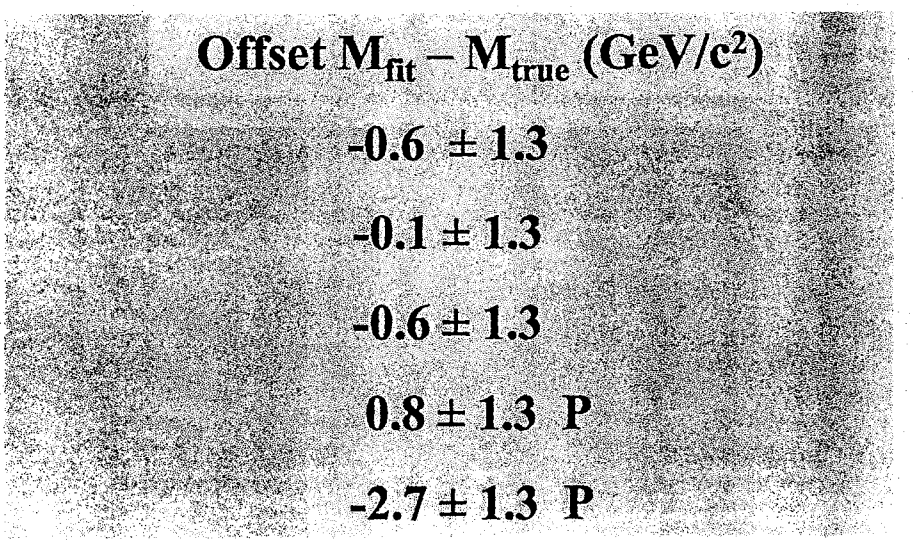

Figure 19: Blind test results.

8 Data

After selecting good runs, the total integrated luminosity for these samples is 335 pb^{-1}.

8.1 Dilepton candidates sample

We performed selection of dilepton candidates. These events are listed in Tab. 1. The examples of pdd's for a few dilepton canididates are presented in Fig. 20.

number	Category	Run	Event	number	Category	Run	Event
1	TCE/CMP	143257	760520	18	CMUP/CMU	166063	2833132
2	PHX/NITCE	150418	960369	19	TCE/NICMX	167053	12011678
3	TCE/NICMP	150431	368759	20	TCE/CMUP	167629	180103
4	TCE/NICMU	150435	2896171	21	TCE/CMX	167631	2058969
5	CMUP/NITCE	151978	507773	22	TCE/CMUP	168599	2964061
6	CMX/CMX	153325	599511	23	TCE/NITCE	177491	3807306
7	TCE/TCE	153374	2276742	24	CMUP/CMIO	178540	2208375
8	CMUP/CMP	153447	2643751	25	CMUP/CMIO	178738	10340757
9	CMUP/CMX	154654	7344016	26	TCE/CMUP	178738	1660363
10	TCE/CMX	155114	478702	27	TCE/CMIO	183963	1259645
11	TCE/CMX	156484	3099305	28	PHX/CMIO	184779	892809
12	CMX/NICMX	160988	385505	29	CMUP/CMP	185037	2287335
13	TCE/CMIO	161633	963604	30	CMUP/CMP	185377	103906
14	CMUP/CMP	162820	7050764	31	TCE/CMIO	185594	3002817
15	CMUP/NICMX	163012	1438203	32	TCE/TCE	186598	1618142
16	CMUP/CMX	165198	1827962	33	TCE/TCE	186598	4194951
17	TCE/CMU	165364	592961				

Table 1: Run and event numbers of the 33 dilepton candidates.

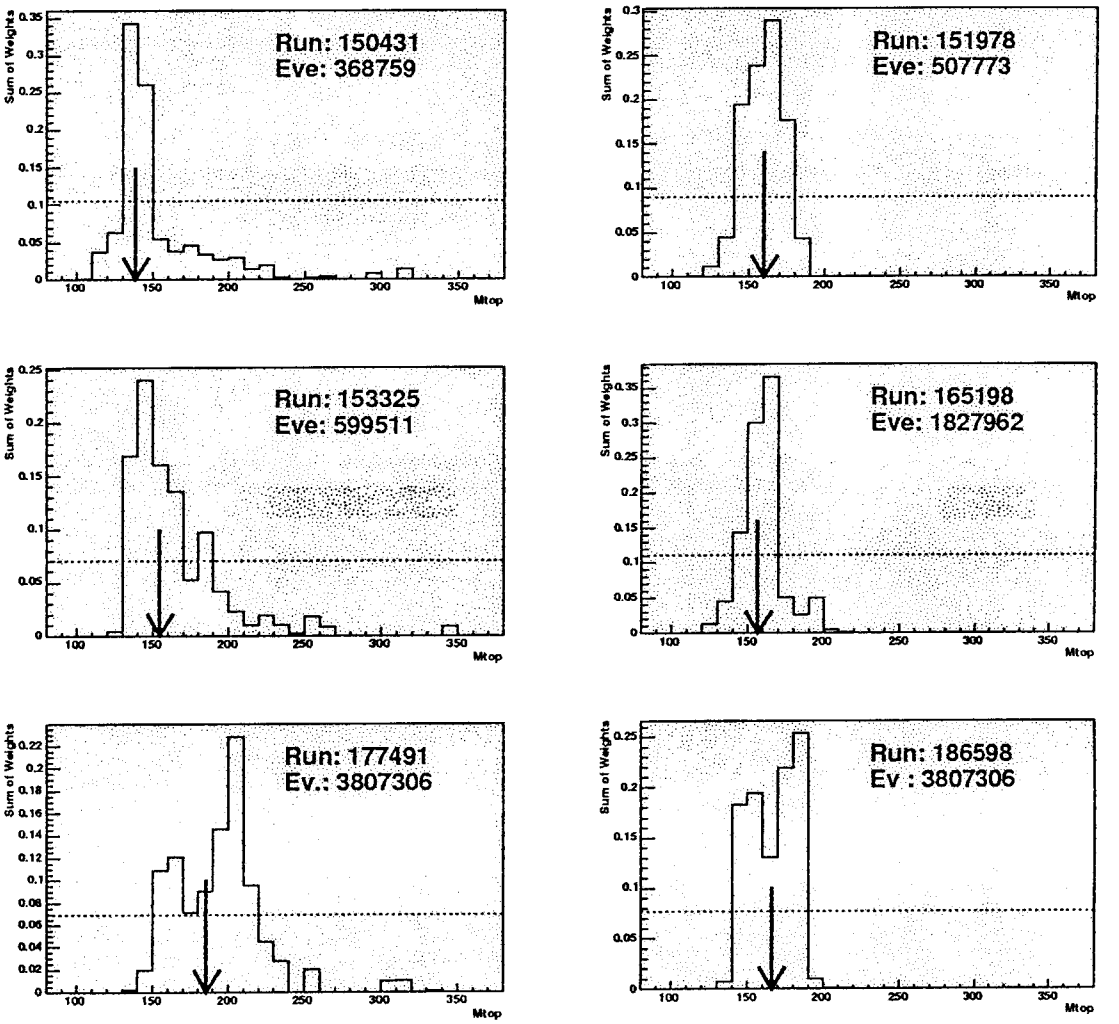

Figure 20: The probability dencity functions for 6 data events. Horizontal lines show our cut at 30% of MPV. The blue arrow indicate the mass taken for the particular event.

8.2 Top mass estimate for the data

The two-component, background-constrained fit (N_b=8.5±1.6) for the obtained dilepton sample returns: $M_{top} = 170.0 \pm^{9.7}_{8.9}$ GeV/c^2, with 25.3±$^{6.2}_{5.6}$ signal events and 8.3±1.6 background events.

The fitted mass distribution is shown in Fig. 21. The insert shows the mass dependence of the negative log-likelihood function.

Expected statistical errors obtained from the pseudoexperiments are shown on Fig 22. The lower plot shows the stat. error distribution for the top mass of 178 GeV ($\sigma_{t\bar{t}} = 6.1$ pb) which is yet the World average top mass. The arrows indicate the errors returned by the fit to the data.

We also performed a fit when the number of the background events was unconstrained. This fit returns $M_{top} = 168.4 \pm^{7.8}_{7.1}$ GeV/c^2, with 33.0±$^{6.1}_{9.6}$ signal events and 0.0±$^{0.0}_{0.1}$ background events.

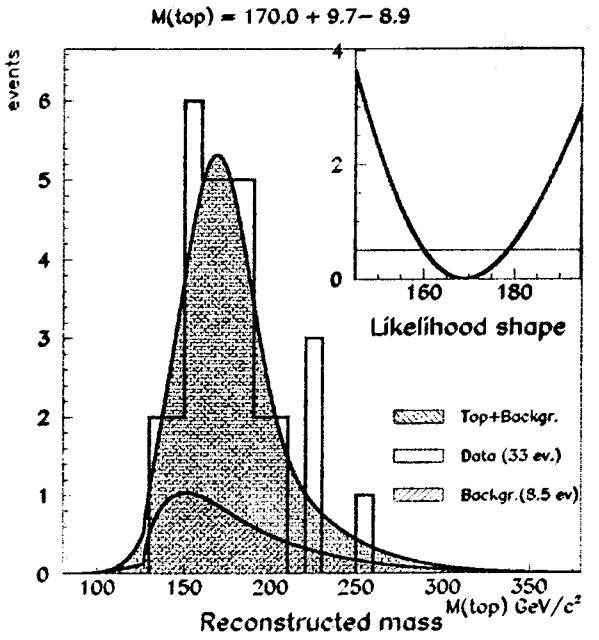

Figure 21: Two-component, constrained fit to the dilepton sample. The violet shaded area corresponds to the background returned by the fit and the red line-shaded area is the sum of background and signal events. The insert shows the mass-dependent negative log-likelihood used in the fit.

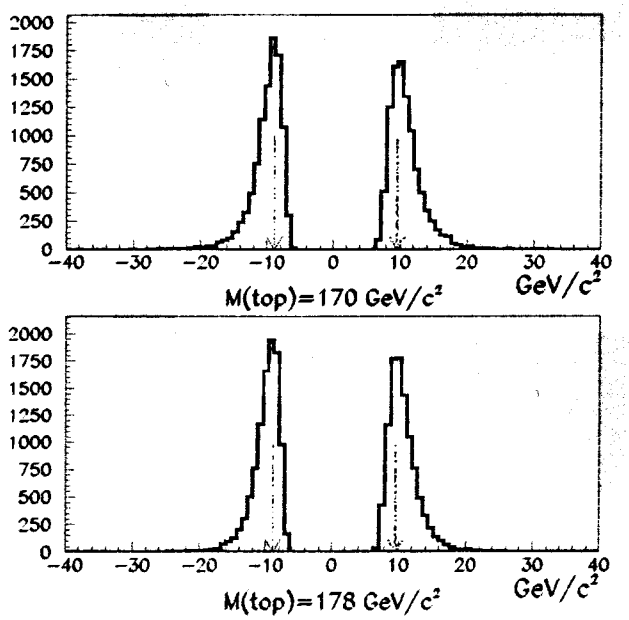

Figure 22: Expected statistical errors for different top masses. The arrows indicate the errors returned by the fit to the data.

9 Systematic Uncertainties

We have considered the following sources of systematic uncertainties on the fitted mass value: a) jet energy scale, b) amount of initial and final state radiation, c) shape of the background template, d) parton distribution functions, and e) approximations made by Monte-Carlo generators, f) limited statistics of Monte-Carlo simulated signal or background samples. The magnitudes of these uncertainties were estimated using large Monte-Carlo samples generated only for the systematics study.

The procedure for estimating the systematic uncertainty is similar for all sources. For each source we varied the input value as appropriate (by 1σ, or changing PDF, etc) and evaluated the impact on the returned top mass. This was done by simulating a large number (usually 10000 or more) of pseudo-experiments (PE) with the nominal assumption and with the alternate assumption. Each PE had the same number of events as in the data. The reconstructed mass distribution from each PE was fitted with the same likelihood procedure as for the data. The obtained mass value was entered into an ensemble of results of simulated experiments. The systematic uncertainty assigned to our measurement is the difference in the average of these result distributions for the nominal and shifted ensembles.

9.1 Jet Energy Scale

In Run 2 the jet systematic uncertainty is included in the jet correction software package. It is possible to turn on a $\pm$ 1σ change in the energy scale for the specific type of jet correction. A

detailed description of each source of uncertainty can be found at Jet Energy and Resolution Group Web Page [5].

By means of the above-described PE we estimated the mass shift caused by different corrections. We obtained the overall uncertainty of 3.4±0.2 GeV shifting jets in both signal and background MC events for jet corrections at levels 1,4,5,6,7 and 8.

9.2 Radiation Effects

The effects of initial (ISR) and final (FSR) state radiation on the returned top mass were studied using Pythia as a signal generator. To estimate the uncertainty induced by ISR we studied the difference between ISR enhanced and reduced samples, as recommended by the top group. The half-difference between average reconstructed top masses from these samples are assigned as a systematic uncertainty from ISR. To estimate the uncertainty induced by FSR we used the Pythia with enhanced and with reduced amount of FSR.

The results for the ISR and FSR induced systematic are summarized in Table 2.

Source		Datasets	Mass GeV/c^2	Mass Shift GeV/c^2
Gen.	Herwig	ttophl	178.6±0.1	1.1±0.2
	Pythia	ttopel	177.5±0.1	
BG Shape	Combined vs. WW-only	ttophl		0.9±0.2
PDF	MRST72 vs. CTEQ5L	ttopir-ttopel		0.2±0.2
	MRST72 vs. MRST75	ttopir-ttopjr		0.3±0.2
	CTEQ6M eigenvect.	ttopel		0.4±0.4
ISR	More ISR	ttopdr, ttoper	178.2±0.1	1.3±0.2
	Less ISR	ttopbr, ttopcr	176.9±0.1	
FSR	More FSR	ttopkr, ttoplr, ttopmr, ttopnr	177.1±0.1	0.3±0.2
	Less FSR	ttopfr, ttopor, ttoppr	176.8±0.1	

Table 2: Top mass shifts obtained from the PE for different Monte-Carlo samples.

9.3 Background Shape

The systematic error induced by the uncertainty in the background shape was assessed by comparing the combined background shape to the the WW background. The result is shown in Table 2.

9.4 Parton Distribution Functions

The uncertainty induced by PDF's was assessed by comparing CTEQ5L vs MRST in Pythia. The difference in top mass was checked also on MRST with two different α_s values (MRST72 with α_s=0.118 and MRST75 with α_s=0.112). The results are listed in Table 2.

The recently developed next-to-leading order PDF from CTEQ6 [9] allows us to vary some PDF sets within their uncertainty. The possible variations are separated into contributions from 20 independent eigenvectors, so in total we have 41 different sets (1 nominal and 2×20 for $\pm 1\sigma$ variations). The PDF effect is studied using the reweighting method [10], where reconstructed top mass templates for each PDF set are obtained from one single sample (Pythia 175 GeV/c^2 sample) by weighting the mass for each event by the probablity for that event to proceed according to the given PDF. Results for the nominal PDF and for the 20 pairs of $\pm 1\sigma$ PDFs are shown in Fig. 23. The black line corresponds to the nominal PDF set. The total CTEQ6M PDF uncertainty was estimated as 0.5 GeV/c^2.

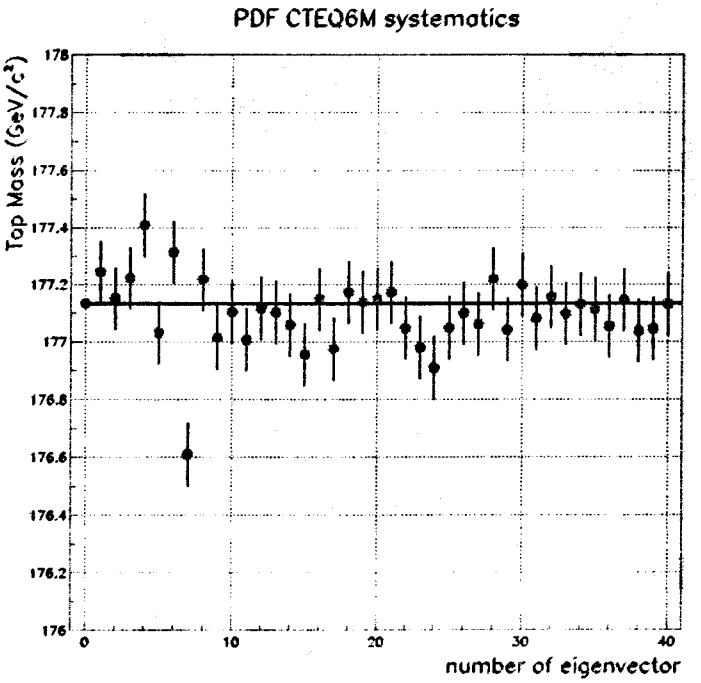

Figure 23: Results used for PDF uncertainty

9.5 Monte-Carlo Generators

The effect of using different top Monte-Carlo generators was checked by comparing nominal Herwig with Pythia samples. The obtained mass shift are presented in Table 2.

9.6 Estimation of Uncertainty from Limited Statistics in Templates

We used the method described in [11] to estimate properly the uncertainty on the median of a mass distribution induced by the limited statistics in templates.

Starting from the initial signal (M_{top}=175 GeV/c^2) or combined background templates we obtained 100 new templates by modeling statistical fluctuation in each bin. The large number of PE (5000 and 10000 for the signal or background cases respectively) were generated with each of these templates. The obtained distributions of medians extracted from the mass distributions for each set of PE are shown in Fig. 24.

In order to isolate the pure uncertanty from the limited template statistics, we subtructed in quadrature the uncertainty due to PE statistics (0.28 GeV/c^2 for the signal case and 0.20 GeV/c^2 for the background case) from the obtained widths. The results are 0.37±0.04 GeV/c^2 and 0.61±0.07 GeV/c^2 for the signal and background templates respectively. We took these values as the uncertainties on the median generated by the limited statistics in our signal and combined background templates. To get correct unceratinties for other signal samples we are scaling the obtained signal uncertainty for the M_{top}=175 GeV/c^2 according to the number of events in these samples.

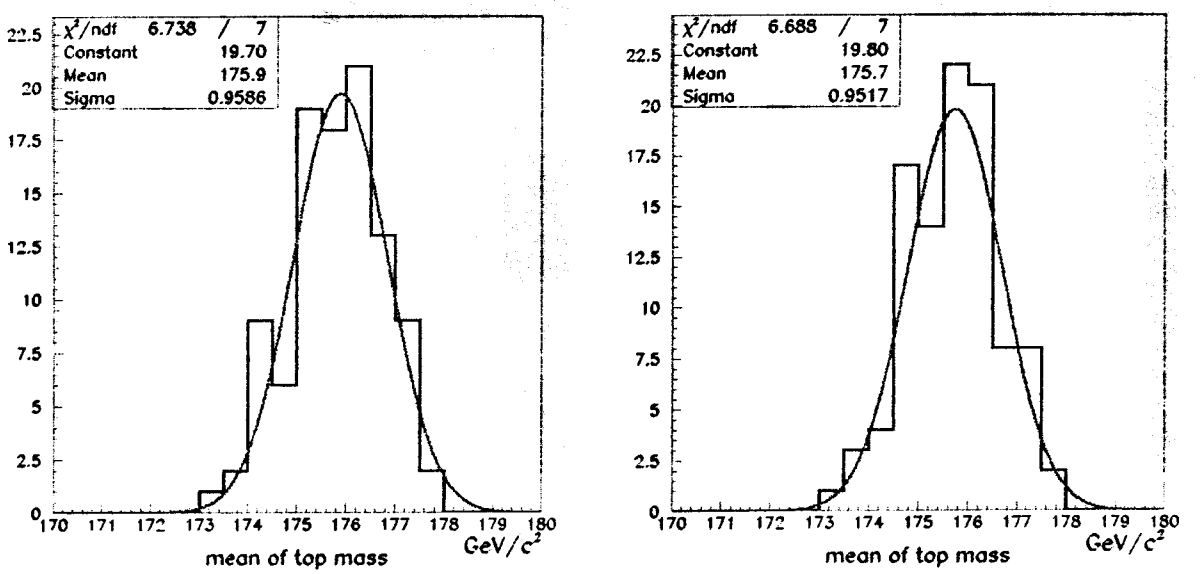

Figure 24: The means of the top mass distributions from 100 sets of the pseudo-experiments generated with the statistically fluctuated signal (left) and background (right) templates.

9.7 Summary of Systematic Errors

The summary of systematic uncertainties are listed in Table 3. For each source of systematic uncertainty we chose the obtained from PE mass shift or its error, which one is bigger.

CDF RunII Preliminary

Source	Uncertainty (GeV/c^2)
Jet Energy Scale	3.4
Initial State Radiation	0.7
Final State Radiation	0.2
Parton Distribution Functions	0.5
Monte-Carlo Generators	1.1
Background Shape	0.9
Limited MC Statistics	1.3
Total	**4.**

Table 3: Systematic uncertainties as determined with the pseudo-experiments.

10 Conclusion

We applied the neutrino ϕ weighting method to solve a non-constrained kinematics of the top quark decay in dilepton mode. 33 candidate events were selected from the data sample with integrated luminosity of $335pb^{-1}$. Our preliminary measurement of the top quark mass in the dilepton sample is

$$M_{top} = 170.0 \pm^{9.7}_{8.9} \text{(stat)} \pm 4.0 \text{ (syst) GeV/c}^2.$$

References

[1] "A determination of the top mass from the dilepton events using the modified lepton+jets MINUIT fitter", CDF note 4607, 1998

[2] "Measurement of the Top Quark Mass with the Collider Detector at Fermilab", CDF Collaboration, Phys.Rev.D63-032003 (2001)

[3] "Summer 2004 Top Mass Measurement in Dilepton Events using the MINUIT Fitter", CDF note 7093, 2004

[4] "Updated Measurement of the Top Quark Mass in the Lepton+Jets Channel",CDF note 6845, 2004

[5] Jet Energy and Resolution Group Web Page at http://www-cdf.fnal.gov/internal/physics/top/jets/corrections.html

[6] "A Measument of the $t\bar{t}$ Cross Section using Dileptons", CDF note 6830, 2004

[7] "Revisiting the Top-Specific Jet Energy Corrections", CDF note 6404, 2003

[8] "Jet Corrections for Top Mass Fitting", CDF note 2469, 1994

[9] J.Pumplin et al., "New generation of parton distributions with their uncertainties with global QCD analysis",hep-ph/0201195

[10] Stephen Miller, http://cdfrh0.grid.umich.edu/ miller/pdf/pdf_acceptance.html, 2004

[11] "Measurement of the Top Quark Mass Using the Template Method by Dividing the Lepton+Jets Sample", CDF note 7139, 2004